Supporting Online Material for

Glioma-Derived Mutations in *IDH1* Dominantly Inhibit IDH1 Catalytic Activity and Induce HIF-1α

Shimin Zhao, Yan Lin, Wei Xu, Wenqing Jiang, Zhengyu Zha, Pu Wang, Wei Yu, Zhiqiang Li, Lingling Gong, Yingjie Peng, Jianping Ding, Qunying Lei, Kun-Liang Guan,* Yue Xiong*

*To whom correspondence should be addressed.
E-mail: kuguan@ucsd.edu (K.G.); yxiong@email.unc.edu (Y.X.)

Published 10 April 2009, *Science* **324**, 261 (2009)
DOI: 10.1126/science.1170944

This PDF file includes:

Materials and Methods
Figs. S1 to S8
Table S1

Supporting online material (SOM)

Materials and Methods

Protein expression and purification. To purify recombinant wild-type and mutant IDH1 proteins, full length human *IDH1* coding sequences were inserted into pRSF-Duet1 vector and were fused in-frame with a HIS tag at the C-terminus. The plasmid was transformed into *E. coli* BL21(DE3)plysS strain and protein expression was induced by addition of 0.6 mM IPTG when cell density reached 0.6 OD600 units. Cells were lysed by sonication and nickel columns (GE Healthcare, USA) were used to purify IDH1-HIS fusion proteins. To obtain IDH1 heterodimer proteins, wild type and R132H mutant IDH1 genes were inserted into a single pRSF-Duet1 vector and tagged with HIS and FLAG at their C-terminus, respectively. Protein expression was induced by IPTG induction. Wildtype:mutant IDH1 heterodimer proteins were isolated by sequential affinity purification using first Nickel resin and then FLAG beads (Sigma-Aldrich, USA).

Gel filtration. Gel filtration was performed using Superdex 200 10/300 GL column (Amersham) on an ÄKATA FPLC system (Amersham). 0.5 ml of 1 mg/ml purified recombinant wild type IDH1 protein and 0.5 ml of 0.26 mg/ml purified recombinant IDH1/IDH1^{R132H} protein complexes were separately loaded onto a Superdex column. Tris-HCl buffer (pH 7.5) was used as mobile phase and protein elution was monitored by UV (280 nm) absorption.

Synthesis of octyl-α-ketoglutarate. The octyl-α-KG ester was synthesized by adapting a published protocol (*10*). Octyl-chloroformate (Sigma-Aldrich) was added drop by drop to a solution of 10 micromolar α-ketoglutaric acid (Sigma-Aldrich) dissolved in equal molar of triethylamine (FLUKA) and 50 ml dichloromethane (Shanghai Chemical Inc.) at ambient temperature. The resulting mixture was stirred at ambient temperature overnight and another 50 ml dichloromethane was added to the solution. The product mixture was washed with 50 ml 0.5 M HCl. Residual water in non-aqueous solution was removed by adding magnesium sulfate powder. The product was obtained after drying in a vacuum.

Cell culture, transfection and treatment. Human HeLa and HEK293T cells were maintained in Dulbecco's Modified Eagle's Medium (DMEM) supplemented with 10% newborn bovine serum, human glioblastoma U-87MG cells were maintained in DMEM medium supplemented with 10% fetal bovine serum. HEK293T cells were transfected by $CaCl_2$ method and HeLa and U-87MG cells were transfected using Lipofectamine (Invitrogen). To mimic hypoxia, $CoCl_2$ treatments were carried out by adding $CoCl_2$ solution into cell culture medium to a final concentration of 200 μM, 4 hours before harvesting. The octyl-α-KG ester treatments were carried out by adding octyl-α-KG ester to the culture medium to the indicated final concentrations 4-6 hours before

harvesting.

Protein structural modeling. Structural analysis and modeling studies of wild-type and R132 mutants IDH1 were carried out using the Coot model-building tools. The structural figures were prepared using PyMOL Molecular Graphics System.

Western blotting. For Western blotting of HIF-1α protein, exponentially growing cells on 90 mm plates were washed with cold PBS once and lysed directly in 1ml SDS loading buffer and heated at 99℃ for 10 min. For Western blotting of other proteins, standard protocol was followed using a 0.5% NP40 lysis buffer (*12*). Antibodies to FLAG (Sigma-Aldrich), HIF-1α (NOVUS BIOLOGICALS, Littleton, CO and Boster Biological Technology, Ltd., Wuhan, China), HIS tag (Cell Signaling Technology, Danvers, MA), to IDH1 (Abcam Inc. Cambridge, MA) and actin (GenScript Corp., Piscataway, NJ) were used.

shRNA knockdown of *IDH1*. RNA sequences for shRNA *IDH1* knockdown were designed using Whitehead Institute for Biomedical Research siRNA Selection Program. Two 21-nucleotide sequences of human *IDH1*, #1 GAAGTCTCTATTGAGACAA corresponding to the coding region and #2 GGGAAGTTCTGGTGTCATA corresponding to the 3'UTR, were selected and cloned into pLentiLox 5.0 vector that also carries a GFP marker. An HpaI and an XhoI restriction site were added to facilitate the cloning. Letiviruses were generated in HEK 293 cells by co-transfection with lentivirus packaging plasmids, pMDLg/pRRE, pRSV-Rev and pMD2.G.

Measurement of IDH enzyme activity and cellular α-ketoglutarate (α-KG) concentration. IDH1 enzyme assays were carried out in the presence of either 4 mM isocitrate, 100 μM $NADP^+$, 2 mM $MnCl_2$ in Tris-HCl buffer (pH 7.5) (*13*) or 30 μM isocitrate, 10 μM $NADP^+$, 2 mM $MnCl_2$ in Tris-HCl buffer (pH 7.5). The production of NADPH was monitored on a HITACH F-4600 fluorescence spectrophotometer. Cellular α-KG concentration was measured enzymatically by modification of published method (*10*). 10^7 U-87MG cells were lysed in 1 ml 0.1% NP-40 Tris-HCl buffer (pH 7.5) on ice for 1 minute and supernatant was collected by centrifugation at 13,000 x g for 15 minutes at 4℃. The supernatant was assayed immediately after centrifugation. To each assay, 10μl 0.5 M NH_4Cl, 50 μl 2mM NADH and 5 units of bovine glutamate dehydrogenase (SIGMA-Aldrich) was added into 300 μl supernatant, the decrease of NADH was monitored on a HITACH F-4600 fluorescence spectrophotometer. A control reaction was carried out identically in parallel with the omission of glutamate dehydrogenase. The α-KG concentration was calculated from changes in fluorescence and was normalized after subtraction of fluorescence value from the control reaction.

Quantitative RT-PCR. The Superscript III RT kit (Invitrogen) was used with random

hexamer primers to produce cDNA from 4 μg total RNA. β−actin was used as endogenous control for samples. All primers for analysis were synthesized by Generay (Shanghai). Primer sequences for each analyzed gene are:
β−actin forward: 5'-TCCCTGGAGAAGAGCTACG,
β−actin reverse: 5'-GTAGTTTCGTGGATGCCACA,
Glut1 forward: 5'-GATTGGCTCCTTCTCTGTGG,
Glut1 reverse: 5'-TCAAAGGACTTGCCCAGTTT,
PGK1 forward: 5'-ATGGATGAGGTGGTGAAAGC
PGK1 reverse: 5'-CAGTGCTCACATGGCTGACT
VEGF forward: 5'-AGGAGGAGGGCAGAATCATCA,
VEGF reverse: 5'-CTCGATTGGATGGCAGTAGCT.
Analysis was performed using an Applied Biosystems 7900HT Sequence Detection System, with SYBR green labeling.

Sequencing of *IDH1* gene in human gliomas. A collection of 26 human glioma samples were analyzed for *IDH1* gene mutation. A portion of the *IDH1* gene exon 4 that encompasses the Arg132 was amplified by PCR using two pairs of primers:
IDH1F1: 5'CGGTCTTCAGAGAAGCCATT; IDH1R1: 5'GCAAAATCACATTATTGCCAAC
IDH1F2: 5'ACCAAATGGCACCATACGA; IDH1R2: 5'TTCATACCTTGCTTAATGGGTGT.
The PCR products were gel-purified and sequenced using the same primer. All 26 samples were sequenced at least twice. 8 tumors were identified to contain a R132H mutation in *IDH1* gene: one case of primary GBM, two cases of secondary GBM, three cases of oligodendroglioma WHO grade II (O II), one case of oligodendroglioma WHO grade III (O III), and one case of astrocytoma WHO grade II (A II) (table S1, fig. S2).

Immunohistochemistry and histopathological analysis. Tissue sections were deparaffinized by xylene two times then hydrated. 0.6% hydrogen peroxide was used to eliminate endogenous peroxidase activity. The sections were blocked with goat serum in TBS for 30 minutes. Sections were then incubated with an anti-HIF1α antibody (Boster Biological Technology, Ltd., Wuhan, China) at 1:500 dilution overnight at 4°C. Secondary antibody was then applied and incubated at 37°C for 1 hour. Sections were developed with DAB kit and stopped with water.

To quantify the HIF-1α positive area in human gliomas samples, five fields (~173 μm^2 each) from each sample were randomly selected and microscopically examined by a pathologist and a neurobiologist in a double-blind manner. Images were captured using a charge-coupled device (CCD) camera and analyzed using Motic Images Advanced software (version 3.2, Motic China Group CO. Ltd). Cells showing either cytoplasmic or nuclear signals (brown) were counted as HIF-1α positive. Cells showing either no signal or weak signal close to the background were scored as HIF-1α negative. The average HIF-1α positive area was calculated by dividing the HIF-1α positively

stained areas over total area. Statistical analysis was performed using seven IDH1 wild-type and seven IDH1 mutated gliomas of similar grade.

Supplement Table 1. *IDH1* mutation in human gliomas

				IDH1	
Patient ID	Patient age(years)	Patient Sex	Tumor Type	Nucleotide	Arg132
374	46	M	secGBM	G395A	R132H
601	42	M	O II	G395A	R132H
356	36	F	secGBM	G395A	R132H
395	41	M	O III	G395A	R132H
917	48	M	A II	G395A	R132H
724	28	M	O II	G395A	R132H
306	44	M	O II	G395A	R132H
013	30	M	prGBM	G395A	R132H
672	36	F	prGBM	WT	WT
289	56	M	secGBM	WT	WT
384	17	M	O II	WT	WT
404	47	M	O II	WT	WT
091	52	F	O II	WT	WT
224	46	M	prGBM	WT	WT
349	26	M	O II	WT	WT
208	46	M	A III	WT	WT
788	50	F	A II	WT	WT
415	80	M	prGBM	WT	WT
487	50	F	prGBM	WT	WT
639	44	M	prGBM	WT	WT
845	9	M	A II	WT	WT
253	50	M	A II	WT	WT
011	73	M	prGBM	WT	WT
690	35	F	O III	WT	WT
863	50	M	O III	WT	WT
144	51	M	prGBM	WT	WT

Total IDH1 mutant patients: 8
Total patients: 26

Fig. S1

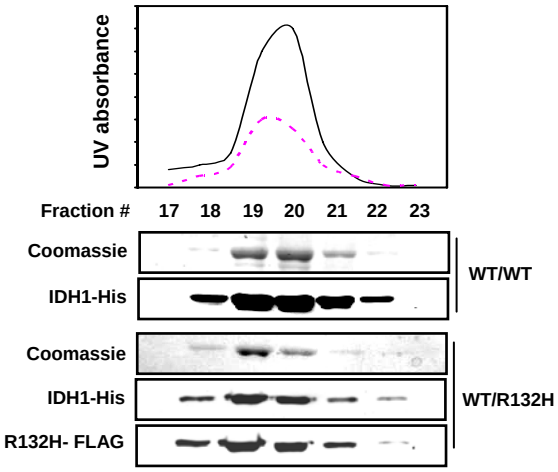

Figure S1. WT and R132H mutant IDH1 forms a heterodimer. Purified recombinant wild type IDH1 protein and IDH1:IDH1^{R132H} protein complexes were separately loaded onto a Superdex column. The wild type IDH1 homodimer was used as a molecular size marker. Tris-HCl buffer (pH 7.5) was used as mobile phase and protein elution was monitored by UV (280 nm) absorption. Black solid line and red dashed line correspond to wild-type IDH1 and IDH1:IDH1^{R132H} heterodimer, respectively. An aliquot from each fraction was separated by SDS PAGE and wild-type and R132H mutant proteins were detected by Western blotting using anti-HIS and anti-FLAG antibody, respectively.

Fig. S2

A

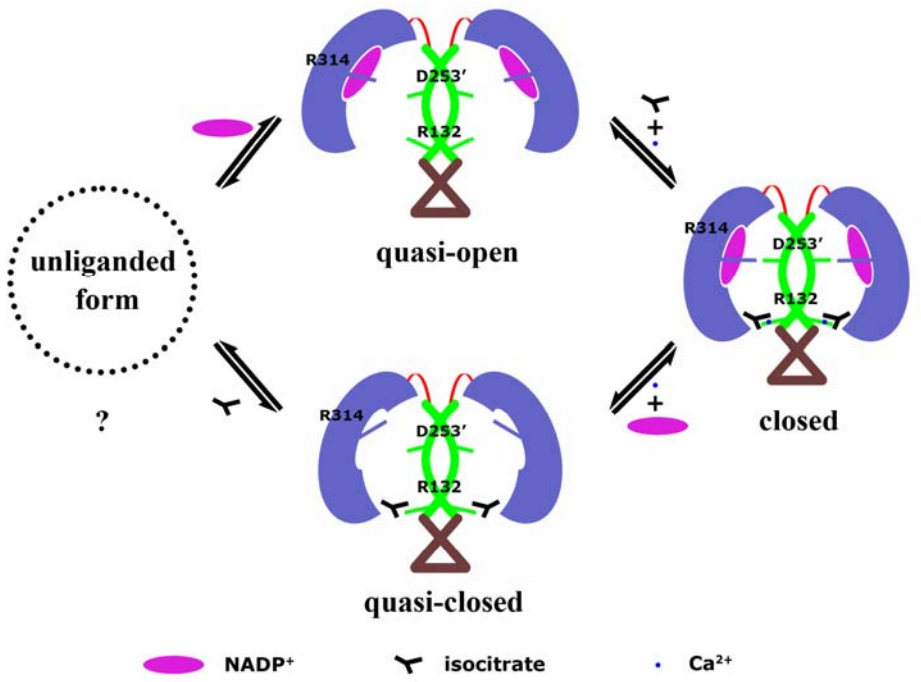
R314
D253′
R132
quasi-open
unliganded form
?
closed
quasi-closed
NADP+
isocitrate
Ca2+

B

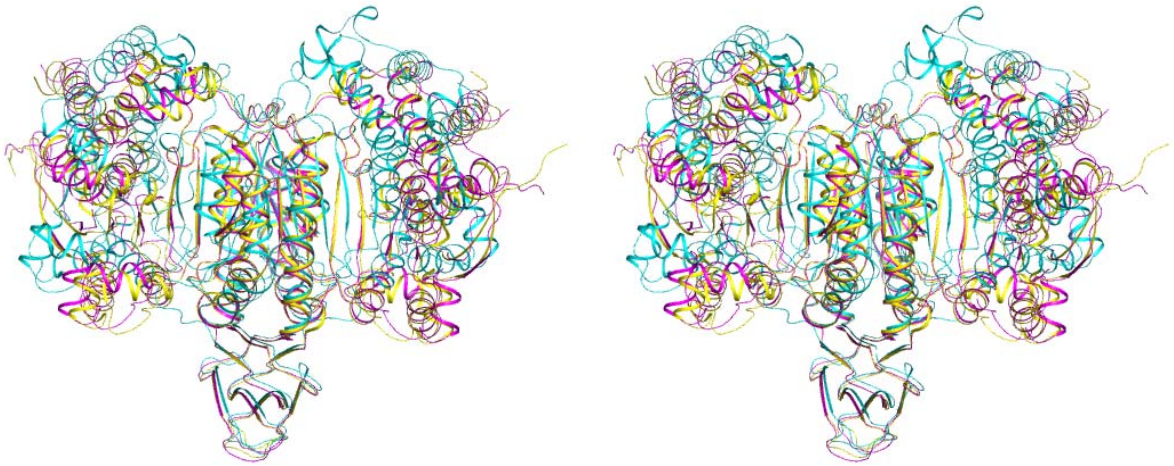

C

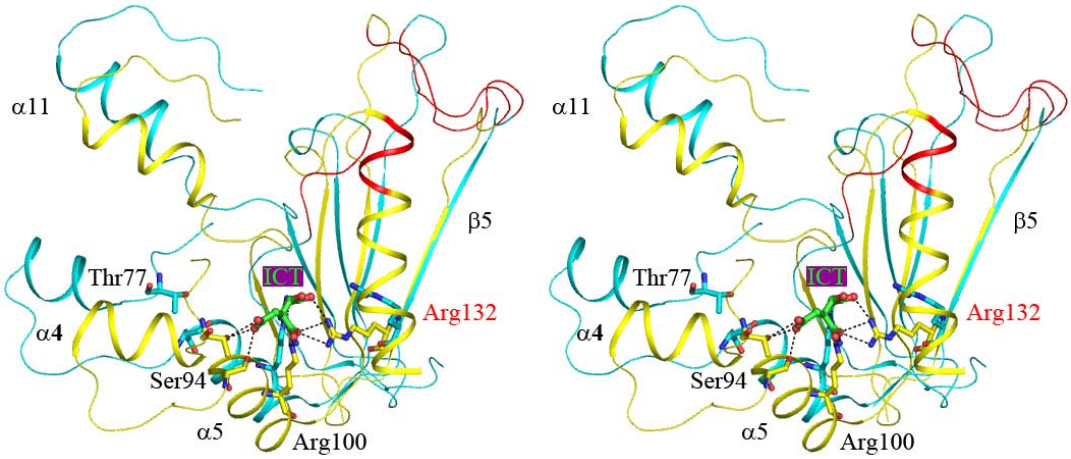
α11
β5
Thr77
ICT
Arg132
α4
Ser94
α5
Arg100

Figure S2. Conformational changes of IDH1 during the catalytic reaction of oxidative decarboxylation of isocitrate. (**A**) A schematic diagram showing conformational changes of IDH1 during the catalytic reaction of oxidative decarboxylation of isocitrate. (**B**) Structural comparison of IDH1 in different enzymatic states showing conformational changes in the overall structure. The enzyme adopts a quasi-open conformation in the IDH1-$NADP^+$ complex (cyan, PDB code 1T09), a quasi-closed conformation in the IDH1-ICT complex (magenta, Yang B. and Ding J., unpublished data), and a closed conformation in the IDH1-$NADP^+$-ICT complex (yellow, PDB code 1T0L). The comparison is based on superposition of the small and clasp domains relative to the IDH1-$NADP^+$ complex. The large domain in the IDH1-$NADP^+$-ICT complex has a 28.8^o rotation towards the small and clasp domains along the hinge regions of residues 117-123 and 282-285 relative to that in the IDH1-NADP complex. The large domain in the IDH1-ICT complex has a 20.7^o rotation towards the small and clasp domains along the hinge regions relative to that in the IDH1-NADP complex. (**C**) ICT (green) binding causes cooperatively conformational changes of the active site. The comparison is based on superposition of the small and clasp domains of IDH1 in complex with $NADP^+$ in the quasi-open conformation (cyan, PDB code 1T09) and in complex with $NADP^+$and ICT in the closed conformation (yellow, PDB code 1T0L). The IDH1-ICT complex in the quasi-closed conformation is omitted for clarity. The hydrogen-bonding interactions are indicated with dashed lines. The large domain in the IDH1-$NADP^+$-ICT complex has a 28.8^o rotation towards the small and clasp domains along the hinge regions of residues 117-123 and 282-285 (red) relative to that in the IDH1-$NADP^+$ complex, leading to the conversion of the enzyme from the quasi-open to the closed conformation.

Fig. S3

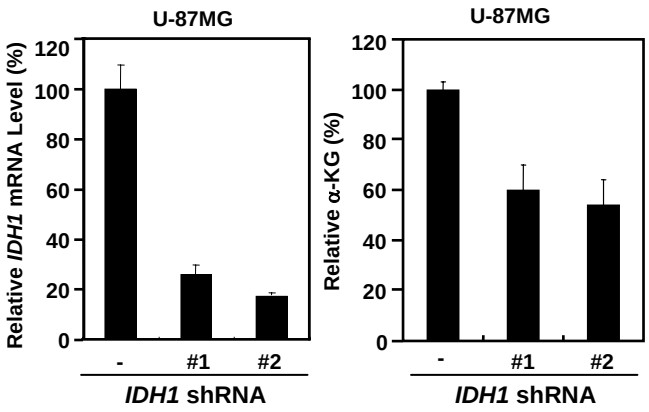

Figure S3. *IDH1* knockdown by shRNA decreases cellular α-KG concentration. Knock down efficiencies of two independent shRNAs were assessed by q-RT-PCR and α-KG levels were determined. Values in control cells were set as 100% arbitrarily and mean values of duplicate assays +/- S.D.

Fig. S4

A

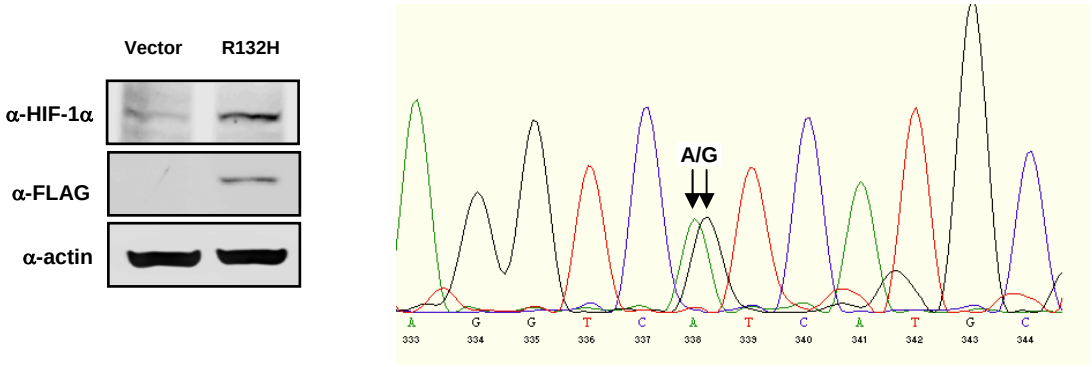
Vector
R132H
α-HIF-1α
α-FLAG
α-actin
A/G
A G G T C A T C A T G C
333 334 335 336 337 338 339 340 341 342 343 344

B

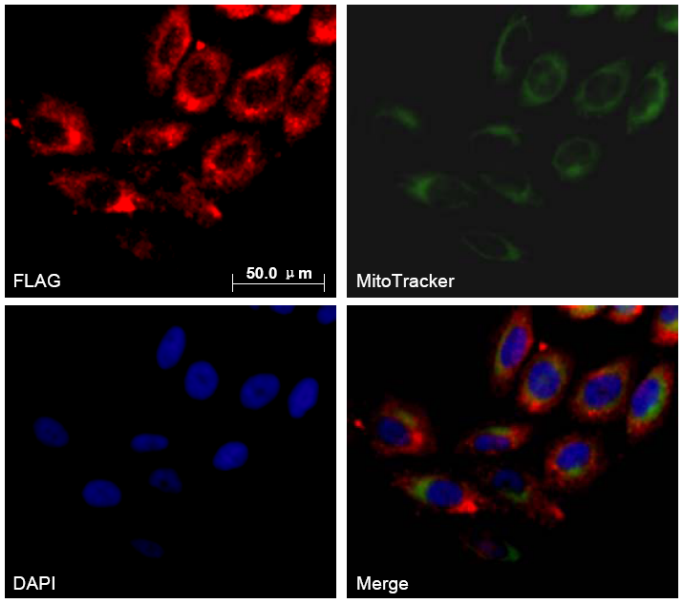
FLAG
50.0 μm
MitoTracker
DAPI
Merge

Figure S4. The levels and subcellular localization of ectopically expressed IDH1^{R132H}

(**A**) To determine the relative level of ectopically expressed IDH1^{R132H} mutant, RT-PCR was carried out using total RNA prepared from stable U-87MG cells transduced with retrovirus expressing IDH1^{R132H}. The expression of FLAG-tagged IDH1^{R132H} and induction of HIF-1α were confirmed by Western blotting (left panel). A pair of primers was used to amplify a 521 bp *IDH1* sequence containing codon R132. RT-PCR products were subjected to direct DNA sequencing to verify the expression of both wild-type and R132H mutant IDH1 (right panel). To quantify the ratio between the wild-type and mutant IDH1 mRNAs, RT-PCR products were cloned into a bacterial vector and 50 independent clones were randomly selected for DNA sequencing. 20 clones corresponded to wild-type IDH1 and 30 to IDH1^{R132H}, indicating that IDH1^{R132H} was expressed at levels of 1.5-folds above that of endogenous IDH1.

(**B**) Ectopically expressed IDH1^{R132H} is localized in the cytoplasm. HeLa cells were transiently transfected with a plasmid expressing FLAG-tagged IDH1^{R132H}. 48 hours after transfection, cells were fixed and stained with an anti-FLAG antibody, a mitochondrion-selective dye (MitoTracker) and DAPI.

Fig. S5

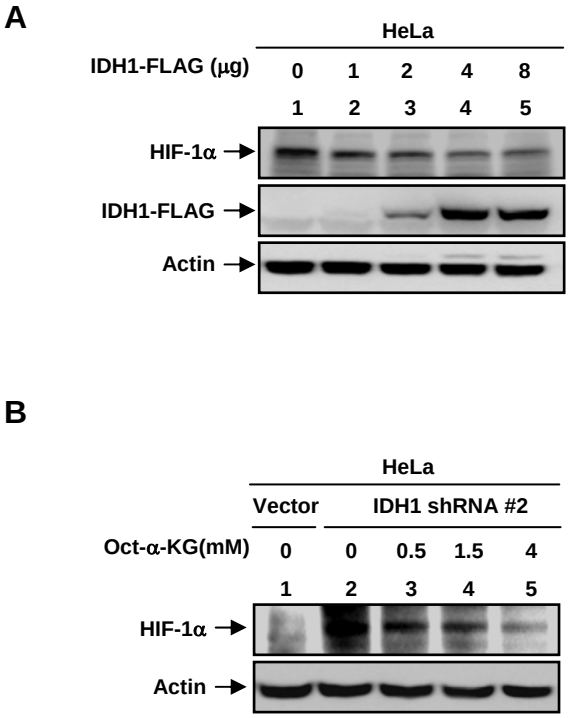

Figure S5. IDH1 overexpression and treatment of cells with a cell permeable α-KG derivative reduces HIF-1α.

(**A**) HeLa cells were transfected with increasing amount of IDH1 expressing plasmid. HIF-1α and transfected IDH1 protein levels were determined by Western blotting using antibody specific to HIF-1α and FLAG, respectively. (**B**) A cell permeable α-KG derivative reduces HIF-1α level in IDH1 knock down cells. Increasing concentrations of octyl-α-KG was added to *IDH1* knock-down HeLa cell culture and steady state HIF-1α levels were determined.

Fig. S6

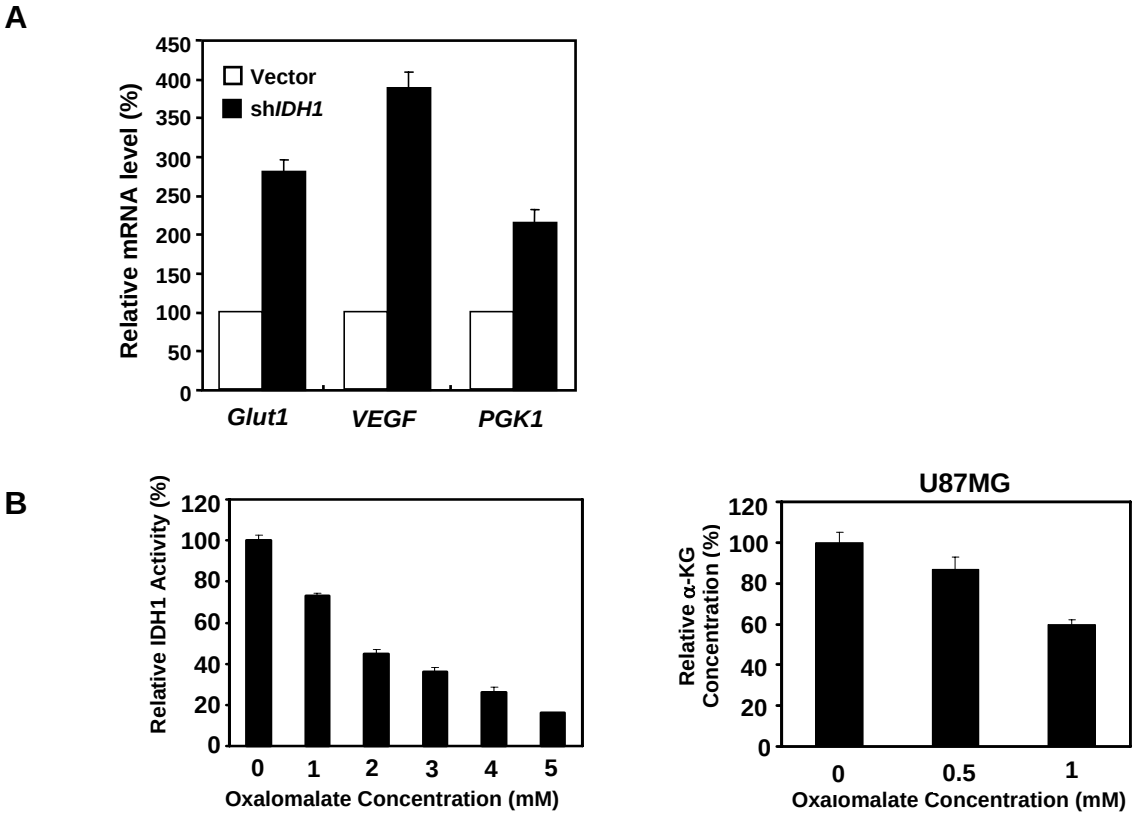

Figure S6. *IDH1* knockdown stimulates the expression of HIF-1α target genes. (**A**) HIF-1α target gene mRNA was determined in U-87MG cells with *IDH1* shRNA #2 or control vector. Levels of mRNAs in shRNA vector infected cells were set as 100%. Shown are mean values of triplicate experiments +/- S.D. (**B**) Oxalomalate inhibits IDH1 and reduces α-KG. Left: The specific activities of IDH1 was measured in the presence of $NADP^+$ (10 μM) and ICT (30 μM), 2 mM $MnCl_2$ and different concentrations of oxalomalate (left panel). IDH1 activity in the absence of oxalomalate was arbitrarily set as 100%. Shown are mean values of triplicate experiments +/- S.D. Right: The α-KG level in untreated U-87MG cells was set as 100% and this value was used to calculate the relative α-KG level in cells treated with different concentrations of oxalomalate. Shown are mean values of triplicate assays +/- S.D.

Fig. S7

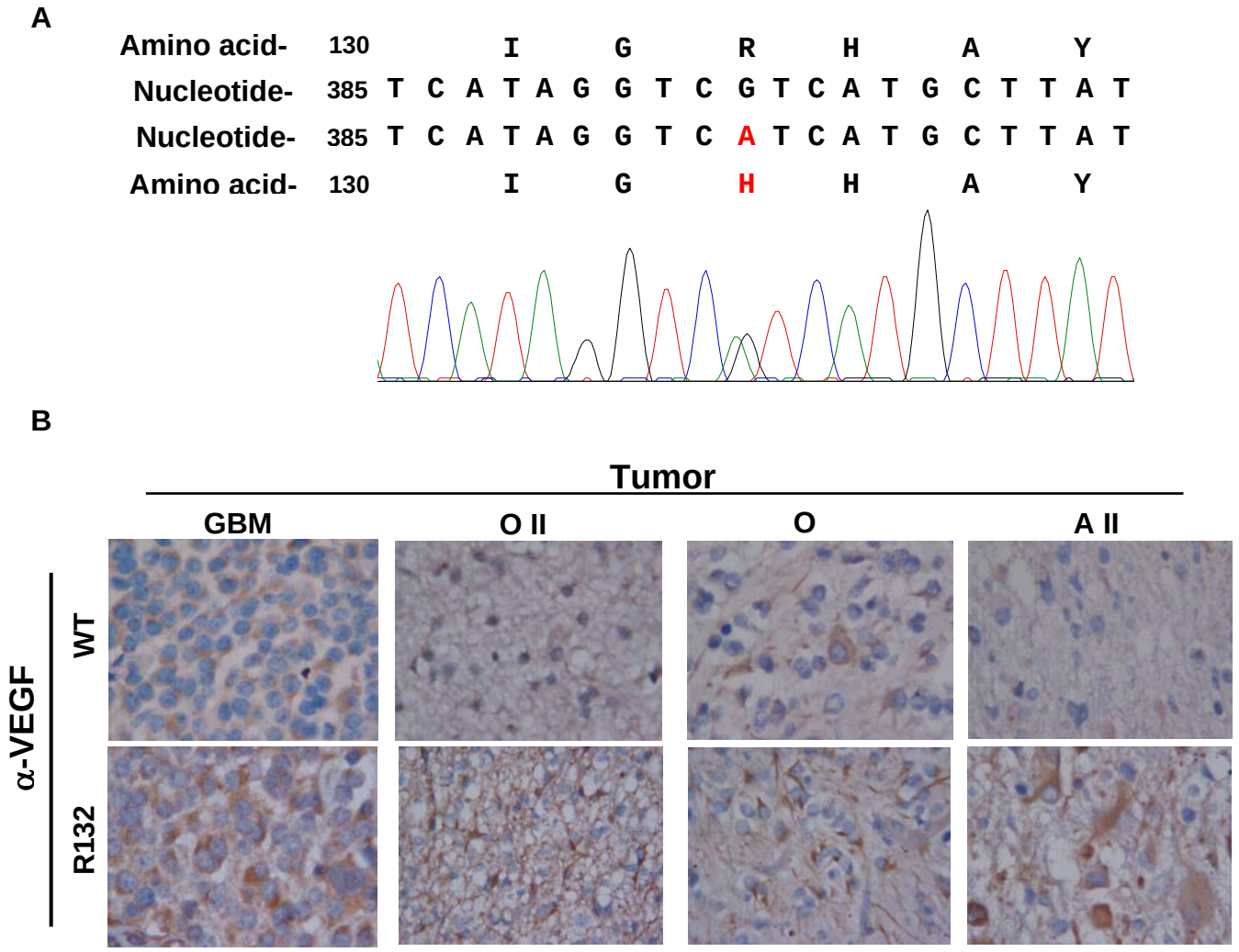

Figure S7. *IDH1* mutations in human gliomas are associated with increased level of VEGF

(**A**) A DNA sequencing example of a R132H mutation in human *IDH1*. (**B**) *IDH1* mutations in human gliomas are associated with increased level of VEGF. Immunohistochemistry of VEGF was carried out in *IDH1* wild-type and mutated gliomas with similar grade. A representative view of 4 tumors of different types or grades is shown.

Fig. S8

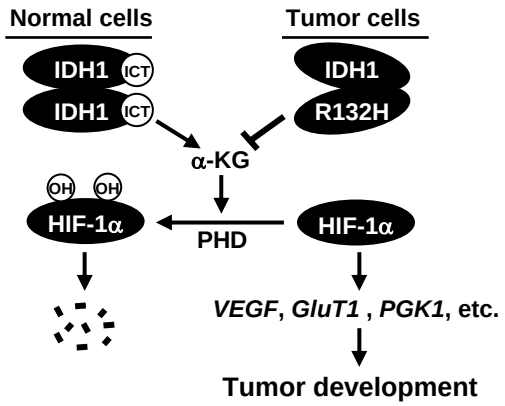

Figure S8. A proposed model for IDH1 as a tumor suppressor. IDH1 normally produces α-KG, which is utilized by PHD to hydroxylate HIF-1α. The hydroxylated HIF-1α is rapidly ubiquitinated and degraded. In tumor cells, mutant IDH1 forms an inactive dimer with the wild type IDH1. Inhibition of IDH1 results in a decreased α-KG level and a decreased HIF-1α hydroxylation, therefore, leading to HIF-1α accumulation and activation of HIF-1 target genes to promote tumor progression.